Drought in the Pacific Northwest, 1920–2013

MU XIAO

Department of Geography, University of California, Los Angeles, Los Angeles, California

BART NIJSSEN

Department of Civil and Environmental Engineering, University of Washington, Seattle, Washington

DENNIS P. LETTENMAIER

Department of Geography, University of California, Los Angeles, Los Angeles, California

(Manuscript received 14 August 2015, in final form 14 June 2016)

ABSTRACT

The severity–area–duration (SAD) method is used in conjunction with the Variable Infiltration Capacity model (VIC) to identify the major historical total moisture (TM; soil moisture plus snow water equivalent) droughts over the Pacific Northwest region, defined as the Columbia River basin and the region's coastal drainages, for the period 1920–2013. The motivation is to understand how droughts identified using TM (a measure similar to that used in the U.S. Drought Monitor) relate to sector-specific drought measures that are more relevant to users. It is found that most of the SAD space is dominated by an extended drought period during the 1930s, although the most severe shorter droughts are in the 1970s (1976–78) and early 2000s (2000–04). The impact of the three severe TM droughts that dominate most of the SAD space are explored in terms of sector-specific measures relevant to dryland and irrigated agriculture, hydropower generation, municipal water supply, and recreation. It is found that in many cases the most severe droughts identified using the SAD method also appear among the most severe sector-specific droughts; however, there are important exceptions. Two types of inconsistencies are examined and the nature of the conditions that give rise to them are explored.

1. Introduction

Drought, which is usually defined as an extended period when water availability is anomalously low in terms of accumulated precipitation (meteorological drought), soil moisture (agricultural drought), or runoff (hydrological drought), can cause large economic losses and inconvenience or suffering to humans. Agriculture, municipalities, hydropower, recreation, and the natural environment all require adequate water. Dilley and Heyman (1995) report that droughts killed 1.3 million people globally between 1967 and 1991. Cook et al. (2007) conclude that drought is the most costly natural disaster in the United States in economic terms. Examples of drought impacts (among many others) include a 25% decrease in Manitoba's hydroelectric production during the 1988 North American drought (Maybank et al. 1995), famine and refugee crises as a result of droughts in the Sahel in the 1980s (Tarhule and Lamb 2003), and losses estimated at around $62 billion (2002 dollars) in the 1988 U.S. Midwest drought (Wang et al. 2009).

The U.S. Drought Monitor (USDM) provides information about current drought conditions across the United States. Although it is based largely on subjective information, NOAA's National Centers for Environmental Prediction (NCEP) provides objective drought information for the USDM based on several land surface models that produce soil moisture estimates, which are converted to probabilities relative to long-term (multidecadal) simulations by each of the models [see Mo and Lettenmaier (2014) for details]. The question

Denotes Open Access content.

Corresponding author address: Dennis P. Lettenmaier, Department of Geography, University of California, Los Angeles, 1255 Bunche Hall, P.O. Box 951524, Los Angeles, CA 90095.
E-mail: dlettenm@ucla.edu

DOI: 10.1175/JHM-D-15-0142.1

we address here is how the droughts identified using these procedures relate to more sector-specific drought measures, which arguably are more appropriate to users of drought information. In this analysis we use total moisture [TM; the sum of soil moisture and snow water equivalent (SWE)] rather than model-based soil moisture, because we believe it to be more appropriate, especially in the western United States.

For the purposes of this study, we define the Pacific Northwest (PNW) region of North America as the Columbia River basin and coastal drainages (Seaber et al. 1987)—essentially USGS hydrologic region 17. It is composed of part or all of seven states in the United States plus part of British Columbia. The PNW has a wide range of climatic and topographic characteristics. It is generally considered a water-abundant region; however, annual precipitation over the region ranges from as little as 200 to more than 2500 mm yr^{-1}. Development of the region's economy was based on abundant water supply (e.g., cheap hydropower used for smelting of aluminum formed the basis for development of the region's aircraft industry and irrigated agriculture is an important economic activity in the interior Columbia River basin). The Cascade Mountains and Rocky Mountains dominate the basin's hydroclimatology through orographic enhancement of precipitation and the natural storage of winter precipitation as snowpack. The region's precipitation is strongly winter dominant, mostly occurring from October to March. Notwithstanding usually abundant water, the PNW region has suffered severe droughts with substantial economic impact over the last 35 years (Shukla et al. 2011). Knapp et al. (2004) found that droughts in the PNW may have regional-scale linkages to the Pacific decadal oscillation (PDO; Mantua et al. 1997) and that some of the recent droughts may be linked to the PDO shift in about 1977 from anomalously cool and wet to warm and dry conditions.

Droughts can be characterized by their severity, duration, affected area, and frequency (Andreadis et al. 2005). Widely used indicators of drought include the standardized precipitation index (SPI), Palmer drought severity index (PDSI), soil moisture deficit index (SMDI), standardized runoff index (SRI), and soil moisture percentiles (SMP) (Palmer 1965; Mckee et al. 1993; Narasimhan and Srinivasan 2005; Shukla and Wood 2008). SPI is an index of accumulated precipitation, whereas PDSI is based on a simplified soil water balance. SMDI, SRI, and SMP are all based on land surface models, which can be of varying complexity.

The USDM uses five drought categories ranging from D0 (least severe) to D4 (most severe), which have been related to some of the above indices (e.g., SMP; Svoboda et al. 2002). Some of the indices noted above have been explored in terms of their performance for regional drought identification. For instance, Shukla et al. (2011) evaluated the ability of SPI, SRI, and SMP to identify the onset and termination of four major droughts in the PNW relative to recorded drought declarations. Andreadis and Lettenmaier (2006) employed monthly SMP and runoff percentiles to study twentieth-century droughts across the conterminous United States.

In this study, we identify the major droughts in the PNW over the period 1920–2013 using TM simulated by the Variable Infiltration Capacity model (VIC) (Liang et al. 1994) and the severity–area–duration (SAD) method of Andreadis et al. (2005). We then evaluate the impact of these drought events on five water-related sectors: dryland agriculture, irrigated agriculture, hydropower generation, municipal water supply, and recreation. The main points of the paper are 1) to evaluate the extent to which droughts identified using regional metrics are evidenced in more sector-specific and local measures and 2) to explore the relationship of these sector-specific and local droughts to the envelope space identified by SAD analysis. We also explore how well (or poorly) the droughts characterized using these methods relate to other drought characteristics in the five sectors noted above of particular interest in the PNW. The remainder of this paper is organized as follows. Section 2 describes the model and forcing data, and section 3 describes the study domain features and SAD method and introduces five sector-specific drought measures. Section 4 reports the results from SAD analysis and the extent to which the major historic droughts identified using SAD analysis do (or do not) match sector-specific drought events over the same historical period. We explore inconsistencies between the regional (SAD based) and sector-specific drought measures in section 5 and end with a summary and conclusions in section 6.

2. Hydrologic model and forcing dataset

We used VIC as our main tool to reconstruct historic droughts. VIC is a macroscale hydrologic model that is based on physical hydrologic processes and parameterizes the effects of subgrid vegetation, topographic, and soils variability on hydrologic processes. The model has been successfully applied in numerous hydrologic studies and water balance simulations. VIC has been updated continually since its inception, and is maintained and archived by the University of Washington (https://github.com/UW-Hydro/VIC).

With respect to drought, Andreadis et al. (2005) used the soil moisture and runoff simulated by VIC to develop the SAD method of characterizing historic

droughts. Andreadis and Lettenmaier (2006) used VIC to study U.S. drought trends in the twentieth century. Wang et al. (2009) used VIC and other land surface models to study characteristics of U.S. droughts, and Wang et al. (2011) used VIC to study trends in droughts in China over the last ~60 years. Mote et al. (2005) employed VIC to study trends in mountain snowpack in the western United States, and Mao et al. (2015) used the VIC output to evaluate the role of climate change in the 2013/14 California drought. We use similar methods to study the nature and impacts of droughts over the PNW over a period of almost 100 years. Our goal here, however, is somewhat different than in the previous studies mentioned above in that we base SAD analysis on VIC TM, then determine how the droughts highlighted by SAD relate to other drought characteristics of the five sectors noted above in the PNW region.

We implemented VIC at 1/16° (~6 km in the north–south direction) spatial resolution using methods and parameters described by Livneh et al. (2013). Specifically, we used gridded daily precipitation, maximum and minimum surface air temperature, and wind speed at a daily time step over the study period 1920–2013. We drew from more than 200 NOAA Cooperative Observer Program stations in the PNW that have long-term and consistent observation records, as described in Wood and Lettenmaier (2006). For the Canadian part of the domain, we used the long-term Canadian stations in the Livneh et al. (2013) dataset. The Canadian stations are relatively sparse and only nine stations have records that are long enough to be suitable for this study. All of the stations we used provide daily observations of precipitation and maximum and minimum temperature. We interpolated the station temperature anomalies for the period 1961–2010 to our 1/16° grid. We then matched the interpolated field anomalies with the grid-based climatology from Livneh et al. (2013) for the years 1961–2010, extended to the entire period 1920–2013 using the same method as in Mao et al. (2015). Precipitation was likewise reconstructed using methods described in Mao et al. (2015). This procedure was intended to capture the spatial variations present in the Livneh et al. (2013) dataset, while tying the long-term variations to the longer-term index stations to avoid spurious trends. The Livneh et al. (2013) dataset uses more stations than we did but many have shorter record lengths, resulting in a dataset that is not as suitable for trend analysis.

Surface wind speed data are not widely available on a station basis, so we used the 1961–2010 long-term climatology calculated from the Livneh et al. (2013) dataset for each individual grid cell. Surface wind speed in the Livneh et al. data were spatially interpolated from the NCEP–NCAR reanalyses (Kalnay et al. 1996) from 1950 onward; earlier in the record, the mean seasonal cycle for 1950–2013 for each grid cell was used. Livneh et al. (2013) assess the errors that result from using the mean seasonal cycle of wind versus time-varying forcings in VIC simulations and show that the effect generally is modest.

3. Approach

a. *Water use in the study domain*

The PNW region is well known for its abundant water, which has been extensively developed for irrigation, hydropower generation, and flood control (Hamlet and Lettenmaier 1999). Most of the precipitation in the region falls between October and March, and seasonal mountain snowpacks supply most of the available water (Ferguson 1999; Hamlet and Lettenmaier 1999). The Columbia River basin covers about 80% of the region aside from coastal drainages to the west of the Cascade Mountains. The seasonal hydrograph of the Columbia River (not accounting for regulation) is typical of snowmelt-dominated streams, with about 60% of the annual discharge occurring between April and July. Much of the region's energy demand is met by hydropower generated at Columbia River dams [60%–70% according to BPA et al. (2001)], and additional hydropower is generated at dams on streams draining the western slopes of the Cascades. Irrigation and municipal water supply also depend on water withdrawals from the Columbia River and its tributaries, although the amounts are modest compared with the main stem Columbia discharge. Two major exceptions are the Yakima and Snake River basins, which supply irrigation water to ~445 000 acres (1801 km^2) and ~2 400 000 acres (9712 km^2), respectively. In both of these two basins, irrigation diversions are about 30% of annual (unregulated) discharge (Vano et al. 2010; Payne et al. 2004).

b. *Identifying total moisture drought*

We ran VIC, version 4.1.2.g, with three soil layers at a daily time step at 1/16° spatial resolution over our study domain (Fig. 1). As in the previous studies noted above, the model was run in water balance mode, meaning that the surface temperature was set equal to the surface air temperature rather than iteratively solving the surface energy budget (the so-called full energy balance mode of the model). For some of the highest-elevation grid cells in areas such as the North Cascades and the Canadian Rocky Mountains, snow accumulated without completely melting in the summer (~1% of the entire region). In reality, some of these areas are glacierized.

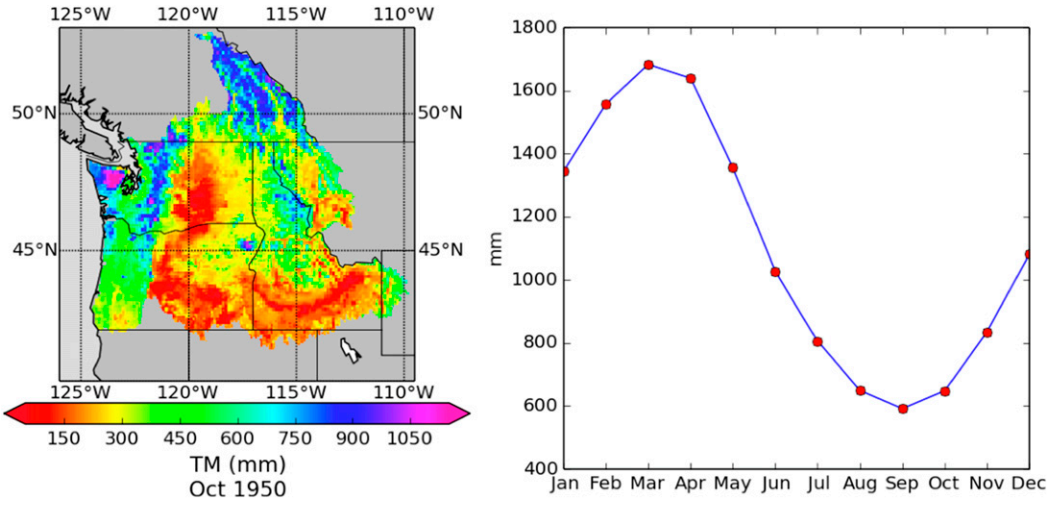

FIG. 1. (left) Study domain with October 1950 average TM from VIC. (right) Long-term average monthly TM from VIC for 47.66°N, 121.28°W.

Because VIC, version 4.1.2.g, does not simulate glaciers, we artificially removed any snow remaining on 1 September of each year. Soil moisture is not much affected because the snow that is removed is in actuality located on glaciers and permanent snow fields. More importantly, the number of grid cells affected is small and has essentially no effect on either the SAD analysis or any of the more sector-specific measures we investigated. Removal of transient initial storage effects was achieved by running the model for 10 years, repeating the first year of the meteorological forcing dataset (1920). The moisture storage at the end of this spinup was then used as the initial state for the 1920–2013 simulation.

The raw model output varies spatially over the region and by season. As an example of the nature of the model's output, Fig. 1 shows the TM over the domain for October 1950 as well as the seasonal variations for one grid cell near the Cascade Mountain crest (47.656 25°N, 121.218 75°W). Both the spatial and temporal variations are apparent. To eliminate the effects of these variations and to provide a universal drought index, a commonly used technique is to interpret the TM as percentiles relative to the model's climatology for a given location and time of year (Sheffield 2004; Mo 2008; Wang et al. 2009). For example, to analyze TM in April 2005, we take all TM April values over 1920–2013 to construct the climatological distribution for each grid cell. The cumulative density function (CDF) of the resulting total moisture percentiles (TMPs) is, by construct, uniform. For any particular value of TM, we can then calculate TMP. This approach has the effect of compensating for model bias, but also "levels the playing field," so to speak, with respect to climatological and temporal variations in TM.

To identify major historical droughts based on TMP data, we used the SAD approach. This method follows Dracup et al. (1980) in defining drought as periods during which TMP is below a threshold. In the SAD method, severity is evaluated based on the average TMP over the drought area. The duration of each drought event is also computed. Grid cells that meet the qualifying criteria are flagged and then a postprocessing spatial analysis is performed that assures spatial contiguity of each event [see Andreadis et al. (2005) for details]. It is important to note that SAD is an envelope method; it does not attempt to attribute frequencies to the events identified and hence is dependent on the specific period of record analyzed [in our work, this is approximately 100 years, and is consistent with the period and data used in Andreadis et al. (2005)]. We used the 20th percentile of TMP as our threshold (equivalent to D1 drought in the U.S. Drought Monitor) and an area threshold of 640 grid cells (~22 400 km^2) as also used by Andreadis et al. (2005). We evaluated drought events with durations exceeding 3, 6, 12, 24, 36, and 48 months.

c. *Regional total moisture drought related to water use sectors*

As noted in section 1, we studied drought impacts on five water use sectors: dryland agriculture, irrigated agriculture, hydropower generation, municipal water supply, and recreation. For each of these sectors, we examined a related hydrological variable and determined the influence of severe droughts (identified using SAD analysis applied to regional TMP) on the sector-specific variable. For dryland agriculture, irrigated agriculture, and municipal water supply, the relevant sector-specific variables can be extracted directly

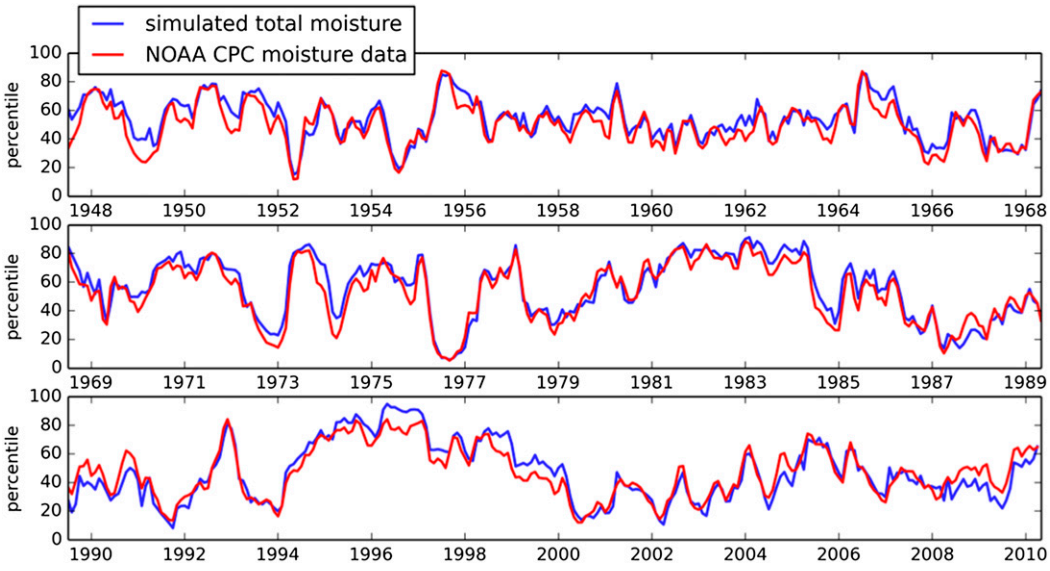

FIG. 2. PNW-average time series of monthly TM percentiles from NOAA CPC (red) and VIC (blue) for 1948–2010. The percentiles were calculated for each model by month and grid cell. The VIC spatial resolution is 1/16°; the CPC spatial resolution is 1/2°.

from VIC (soil moisture and streamflow). For hydropower generation, we used the Columbia Simulation (ColSim) reservoir model of Hamlet and Lettenmaier (1999) to calculate annual hydropower generation based on streamflow predicted by VIC. ColSim simulates reservoir operations, including hydropower generation, using VIC streamflow routed to a set of input nodes in the headwaters of the Columbia River and its major tributaries. It has been applied in several studies of climate change impacts on the PNW region (Hamlet et al. 2002; Payne et al. 2004; Markoff and Cullen 2008; Lee et al. 2011). The model simulates the most important aspects of the Columbia River system water management policy, including hydropower generation, and it is reasonably accurate in emulating the operational decision effects. With respect to recreation, we focused on skiing at several sites in the region. For this purpose we used VIC's snow depth output as an index.

4. Results

a. Model evaluation

For purposes of evaluation, we compared TMP from VIC with soil moisture from NOAA's Climate Prediction Center (CPC), which is produced by a simple bucket model run globally at 0.5° spatial resolution. It does not separate solid water (ice and snow) from liquid water (Fan and Van den Dool 2004). Arguably, it is therefore most appropriate to compare VIC TMP with the CPC moisture values (converted to percentiles). Figure 2 shows time series plots of the two for the period 1948–2010 (the CPC product is not available prior to 1948). The two time series are remarkably similar given differences in models and datasets, and in fact are more similar than comparisons of five different land surface models for the western United States shown by Wang et al. (2009). The VIC simulation results have the same general variations, and extremely low TMP values occur at about the same time.

Figure 3 shows VIC-simulated seasonal streamflow percentiles plotted against the naturalized flow for the Columbia River at the Dalles, Oregon (adjusted from observations, and hence independent of the model output). The naturalized flow data are from the Columbia River Management Joint Operating Committee (2015) "no regulation, no irrigation flows" data provided by Bonneville Power Administration (http://www.bpa.gov/power/streamflow/default.aspx). The points are tightly scattered around the 1:1 line, with a correlation coefficient of 0.95. These results suggest that the VIC streamflow is a good index of the best estimates of streamflow at the Dalles in the absence of water management effects. In the absence of large-scale soil moisture or TM observations, the streamflow results give confidence that VIC TMP is hydrologically realistic.

b. Regional drought identification

Figure 4 shows the envelope curves for SAD analysis over the PNW domain using monthly TMP inputs. Different marker shapes correspond to different drought durations (3, 6, 12, 24, 36, and 48 months) and

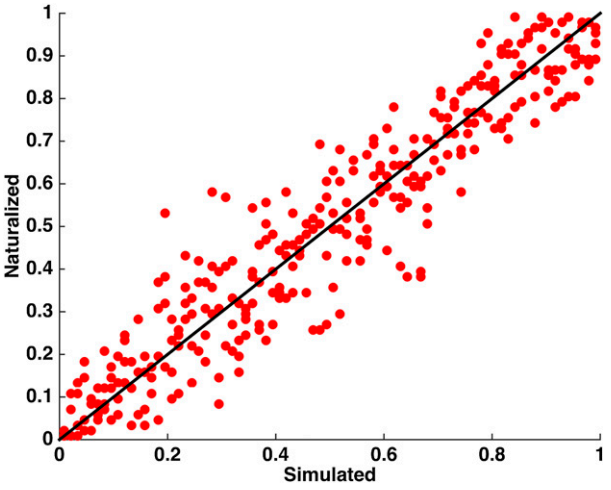

FIG. 3. Scatterplot of VIC-simulated seasonal streamflow percentiles vs naturalized seasonal streamflow percentiles for Columbia River at the Dalles from 1920 to 2013. The correlation coefficient is >0.94.

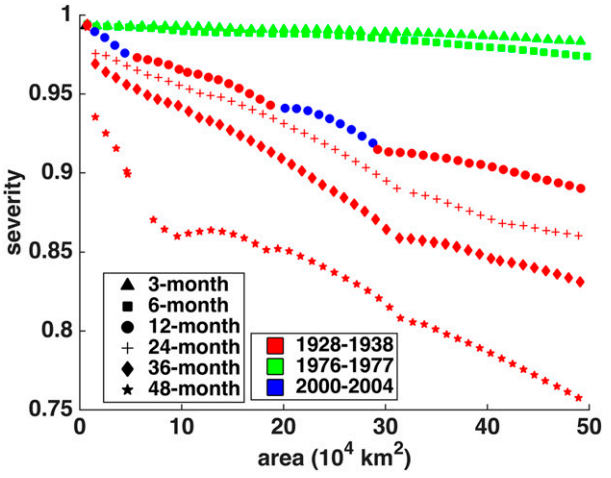

FIG. 4. SAD analysis envelope curve results for the PNW. Each point shape represents one duration (3, 6, 12, 24, 36, and 48 months). Colors correspond to different drought events.

different drought events are color coded. The *x* axis is the area affected by each subperiod in those major drought events, and the severity along the *y* axis is computed as 1 minus average TMP/100 in the affected area. For a more detailed explanation of the method, the reader is referred to Andreadis et al. (2005). Three time periods dominate the plot: the 1930s (from September 1928 to June 1938; red), 1977 (from November 1976 to December 1977; green), and the early 2000s (from January 2000 to November 2004; blue). The 1977 drought is the most severe for the shortest durations (3 and 6 months) considered. The drought events of the 1930s (red) occupy more than half of the points on the plot. The most severe two years of this drought are 1930 and 1935. The early 2000s drought populates part of the 1-yr envelope curve.

Spatial plots of TMP for four selected months (November 1929, February 1937, July 1977, and November 2002) are shown in Fig. 5. Each of these months is within one of the major drought events as determined by the SAD analysis. In each of these months, large areas of the study domain had extremely low TM compared with the 1920–2013 medians.

c. *Sector-specific consistency with the SAD droughts*

The SAD results (section 4b) indicate that there are 16 water years that are within major TM drought periods (of varying durations and areal coverage). We investigate here the relationship between sector-specific droughts and the regional droughts in these 16 water years, and in particular the consistency, or lack thereof, between droughts identified using the regional TM-based SAD analysis and the sector-specific measures we identify below. Inconsistencies between the sector-specific indices and the SAD-based events can be grouped into two types: 1) severe sector-specific events that are not among the 16 SAD-based years (we define a threshold for sector-specific events as cumulative probabilities less than 0.2, i.e., the 20% of years with the most severe indices) and 2) SAD-based years for which there is no corresponding severe sector-specific event. We denote these as type 1 and type 2 inconsistencies below.

We investigated the impact of soil moisture drought on wheat production as representative of the dryland agriculture sector. The link should be direct because wheat growth depends on soil moisture during the growing season (during that period, TM is essentially equal to soil moisture, and we refer hereafter to the dryland agriculture index as TM rather than soil moisture). According to USDA (1997), wheat grows mainly from March to August in the PNW (winter wheat), and we therefore focus on that time period. The counties that are responsible for most of the production of wheat in the PNW are shown in Fig. 6. Given this information, our index is the average March–August soil moisture over the 18 selected counties. Figure 7 shows the March–August TM indices of the most severe year during each major total moisture (SAD) drought identified above, with type 1 and type 2 inconsistencies color coded. The three black horizontal lines correspond to the 5th, 10th, and 20th percentiles of the TM index for the dryland region; the climatological mean of the index is shown as well. Nearly half of the SAD events (7/16) are below the 20th percentile of TM for the dryland region, including four years in the 1930s,

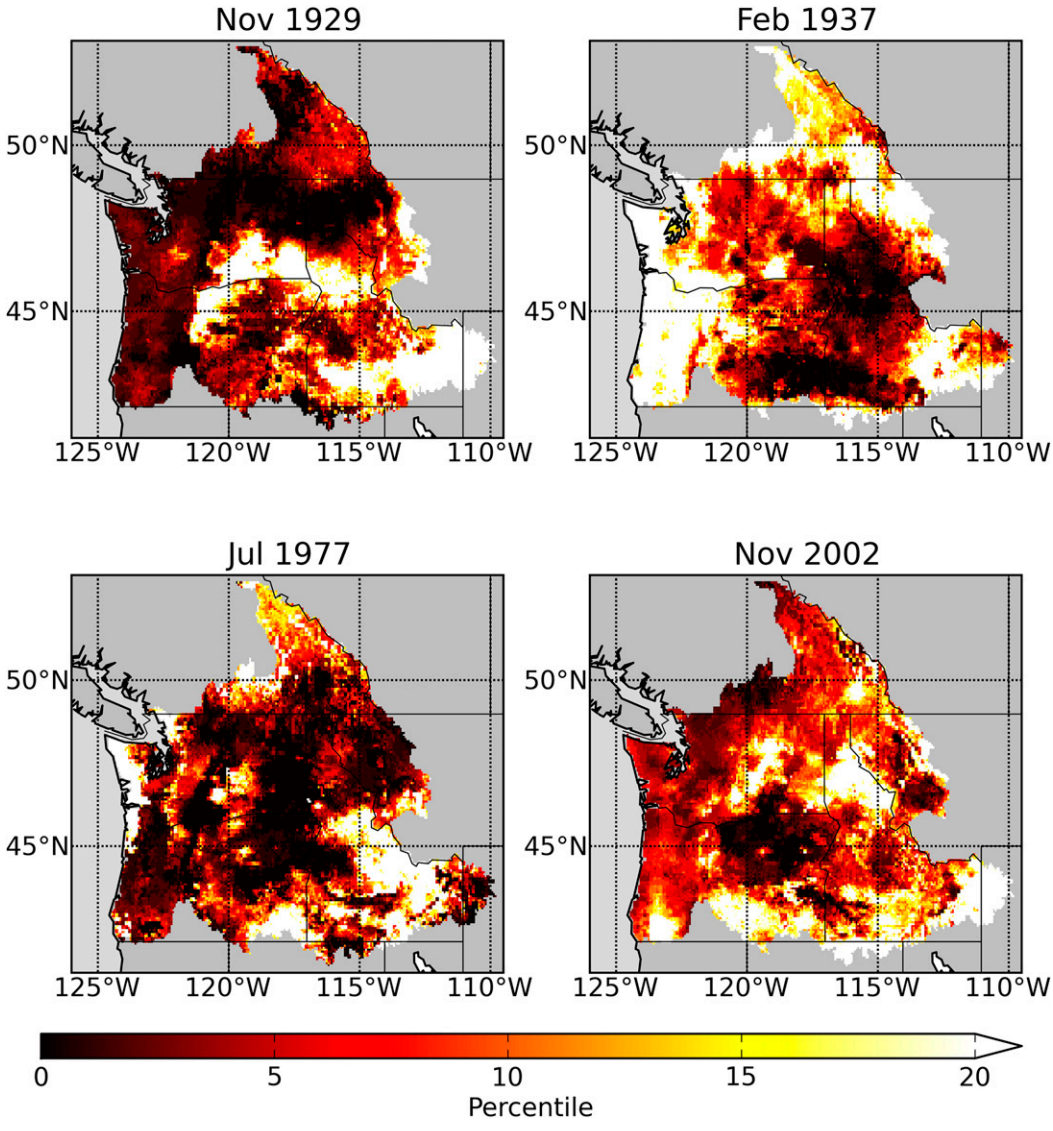

FIG. 5. Spatial plots of selected months within four severe droughts (as TM percentiles) identified by SAD analysis over the PNW.

1977, and two years in the 2000–04 drought period. Eleven years fall below the 20th percentile of the sector-specific index but are not among the SAD drought years (type 1 inconsistency). Most of the type 1 events are not extremely severe in terms of the sector-specific index; three of the four most severe sector-specific events are also SAD drought years. The two most severe type 1 events are 1992 and 1988. Nine SAD years do not fall below the 20th percentile of the sector-specific index (type 2 error).

About 50% of the irrigated agriculture in the PNW is in the upper Snake and Yakima River basins. Two-thirds of the upper Snake River irrigation area receives its water directly or indirectly (the latter via the Snake River Aquifer) from surface water discharge in the basin, and almost all of the Yakima River basin's irrigation water comes from surface water (Vano et al. 2010). We used the water-year river discharge (naturalized, i.e., the discharge that would have occurred in the absence of irrigation diversions) in these two basins as indices for the effect of drought on irrigated agriculture. Figure 8 shows irrigation drought indices for the SAD years as well as years corresponding to type 1 and type 2 inconsistencies for both the Snake and Yakima River basins. For the Snake River basin, seven of the SAD events are below the 0.2 sector-specific threshold, and six are below the threshold for the Yakima basin, with 10 and 11 type 2 events for the two basins, respectively.

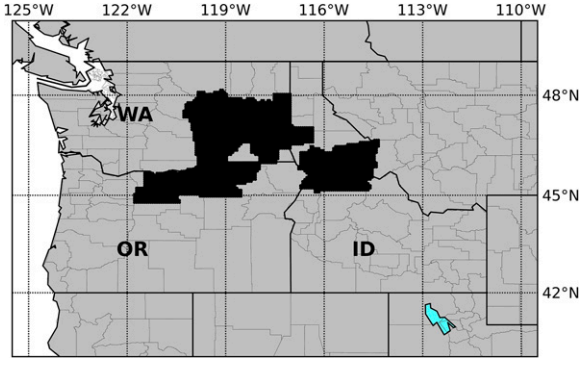

FIG. 6. Major wheat-growing counties in the PNW, defined as having long-term annual average wheat production greater than 3 million bushels (from USDA National Agricultural Statistics Services; http://www.nass.usda.gov/).

However, the SAD-based years account for three of the four most severe drought years for the Snake River and four of the five most severe for the Yakima basin. On the other hand, several of the type 2 years have irrigation drought indices that exceed the median for the Yakima River basin.

The ColSim model simulates hydropower generation at the major Columbia River reservoirs. We used the ColSim energy outputs as our index for hydropower. ColSim is forced by monthly naturalized (formally "adjusted" to a common level of irrigation withdrawals) streamflow routed from the VIC runoff field [using the method of Lohmann et al. (1998)]. Figure 9 shows the hydropower indices; all four of the most severe events are SAD years (2001/02 has the lowest hydropower generation), and nine of the 18 years below the 20th percentile of the hydropower index are SAD years. However, 1977, which is associated with the most severe sector-specific index for the other four sectors, is not among the 18 years below the 20th percentile of the hydropower index. Furthermore, among the seven type 2 years, two have hydropower indices that exceed the median.

To evaluate droughts in the water supply sector, we focused on four cities west of the Cascade Mountains and studied the rivers that provide most of their municipal water supply: Portland (Bull Run River), Seattle (Cedar River), Tacoma (Green River), and Everett (Sultan River). A distinguishing feature of all of these rivers is that they are small, with drainage areas of several 100 km^2 each. We used the average total (annual) runoff for each basin as our municipal water supply index. The relationships with the drought year indices are plotted in Fig. 10. Of the 18 years below the 20th percentile for the municipal water supply index, four were from SAD years at Bull Run, and six at each of the other three basins. In all cases, the most severe drought year according to the water supply index was an SAD year (1977 in the case of Bull Run, and years in the 1930s at the other three). Several type 2 years (SAD years with water supply indices that exceeded the 20th percentile) were above the median water supply index.

Finally, we selected three ski areas to study the relationship between regional drought and winter recreation in the PNW. The ski areas selected were Sun Valley (Idaho), Mt. Bachelor (Oregon), and Stevens Pass (Washington). The most important factor that controls skiing activity is snow depth, with a minimum operational threshold of about 30 cm (Scott et al. 2007; Steiger and Stötter 2013). Accordingly, we defined our index as the number of days in each water year during which the snow depth exceeded 30 cm. The indices for SAD events and those years below 20% threshold are shown in Fig. 11. The 1977 drought is associated with the most severe index of record at Sun Valley and Mt. Bachelor, but not at Stevens Pass. On the other hand, only 3/18 severely low snow years at Sun Valley, 6/18 at Mt. Bachelor, and 8/18 at Stevens Pass were SAD years; hence, both type 1 and type 2 mismatches were highest of any of the sectors. Also, as many as half of the type 2 years had snow indices that exceeded the median.

5. Discussion

Our analysis shows that the most severe regional (SAD) droughts in the Pacific Northwest during the

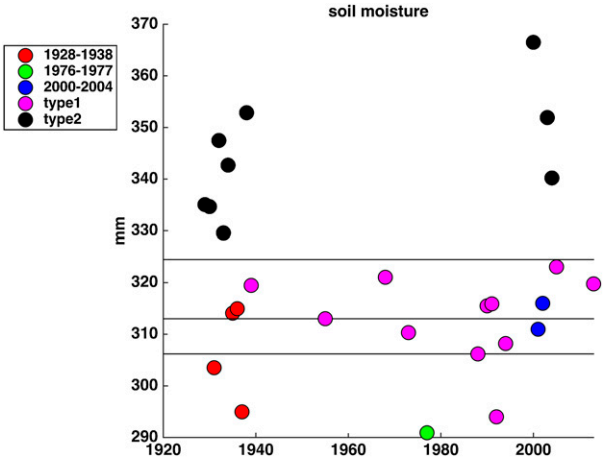

FIG. 7. March–August-average soil moisture over the selected major wheat-growing counties in Fig. 5. Each colored circle corresponds to one of the four most severe regional soil moisture droughts during the period of analysis from regional SAD analysis. Type 1 and type 2 events are defined in section 4c.

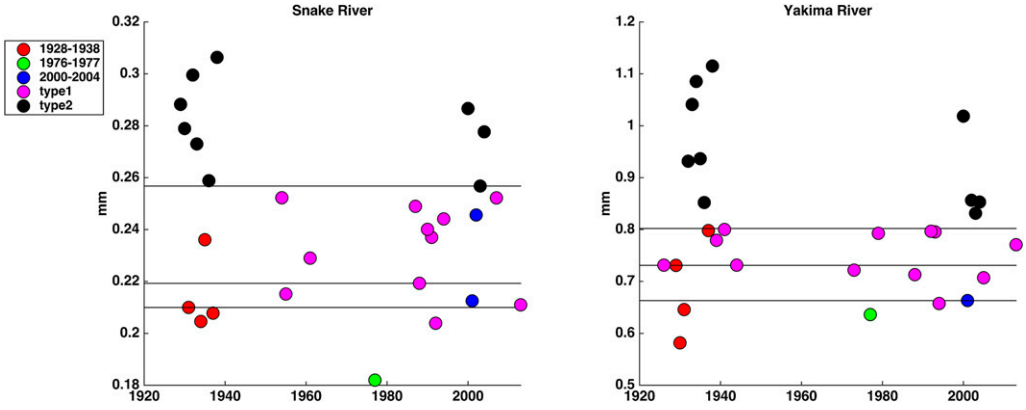

FIG. 8. As in Fig. 7, but for average (water year) runoff over the (left) upper Snake River basin and (right) Yakima River basin.

period 1920–2013 occurred during the 1930s (Dust Bowl), 1970s, and the early 2000s. Our results in this respect are consistent with those of Shukla et al. (2011), Wang et al. (2009), and Andreadis et al. (2005). While there is some consistency among the sector-specific and regional droughts, there are important differences, which we explore here in terms of characteristics of type 1 (sector-specific drought not among the SAD drought years) and type 2 (SAD drought year not among the sector-specific droughts) inconsistencies. The relationship between the sector-specific drought measures we used and the TM variable used in the SAD analysis doubtless is responsible for some of the similarities: four of the five sector-specific indices are strongly related to TM percentiles (the exception is hydropower generation). Even so, spatial differences can lead to different specific events being identified in the most severe sector-specific and regional groups.

Table 1 summarizes the commonality of each sector index and the 16 SAD years. We constructed the distribution of the sector-specific indices for the study period (1920–2013) and then the fraction for the three categories (<5%, <10%, and <20%) that were associated with SAD-based (regional) events. For irrigation, municipal water supply, and recreation, there is more than one site (two, four, and three, respectively). Therefore, for these sectors the total numbers of SAD events considered were 32, 64, and 48, respectively. As noted above, the recreation index has the least commonality between the SAD and sector-specific index (although the 1977 drought is associated with the most severe sector-specific index at two of the three sites). The other four indices show more overlap. Hydropower generation and dryland agriculture have the highest consistency fractions (9/16 and 7/16). Nonetheless, the severe one-year 1977 drought, which is prominent in the other four sectors, does not appear among the hydropower droughts, likely because the operating policy for Columbia River hydropower generation includes a presumption of multiyear droughts and uses stored water in the reservoir system to modulate the effects of low flows in individual years (Hamlet et al. 2002). We explore this hypothesis further below.

For dryland agriculture, we used a TM index that, while specific to the major wheat growing areas rather than the entire region (and for the growing season rather than the entire year), is basically the same as TMP used in the SAD analysis. To analyze the inconsistency further, we computed the local mean TM anomaly for the wheat-growing region for type 1 (~−55 mm) and type 2 (~−10 mm) events. The fact that the type 1 events have relatively large negative anomalies while type 2 events have small (in absolute value) anomalies suggests that the inconsistency between SAD and dryland agriculture events (type 1 vs

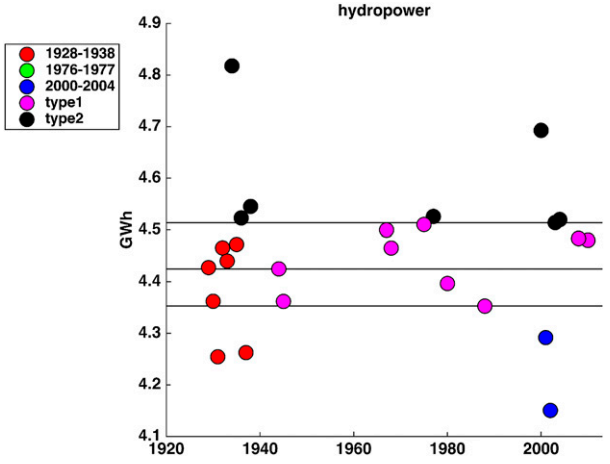

FIG. 9. As in Fig. 7, but for annual hydropower generation in the PNW.

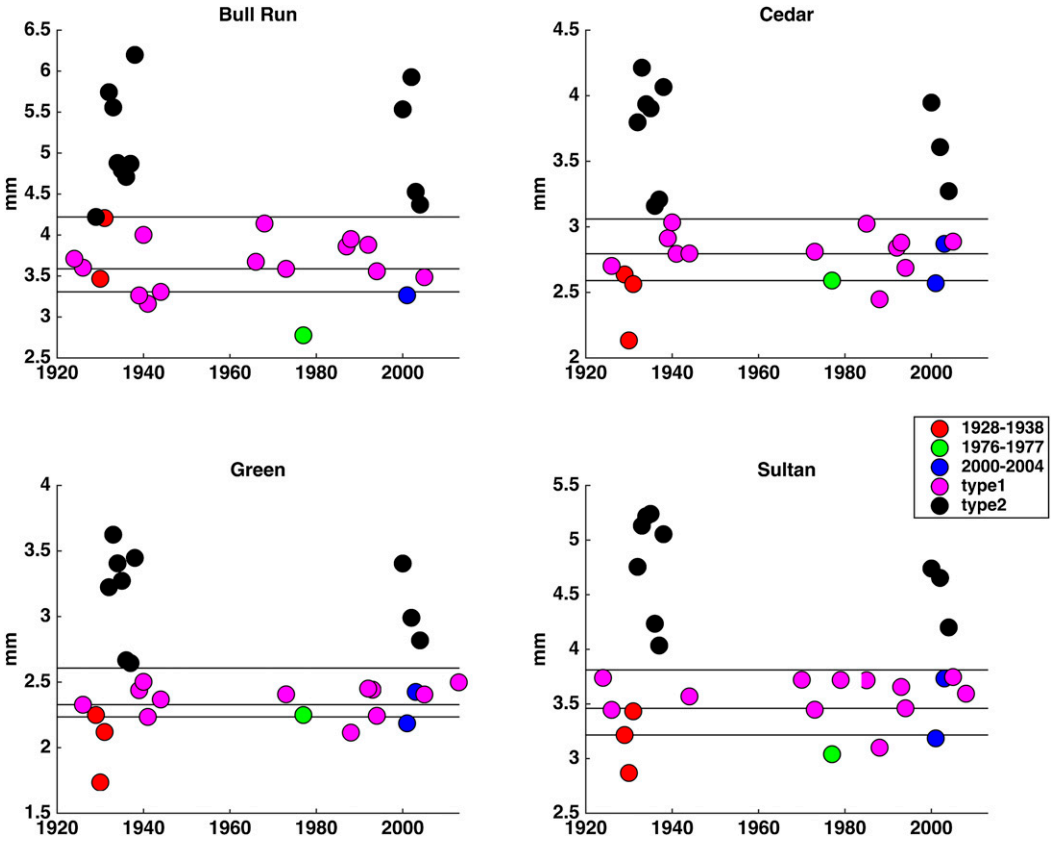

FIG. 10. As in Fig. 7, but for average annual runoff for (top left) Bull Run River, (top right) Cedar River, (bottom left) Green River, and (bottom right) Sultan River.

type 2) has to do with differences between local (wheat growing area) and regional TM and/or differences in growing season versus annual TM.

For irrigated agriculture, we examined, for both river basins, the SWE anomalies on 1 April, which is an indicator of water storage during the winter that will be available for use as irrigation water during the growing season. The anomaly bar plots are shown in Fig. 12. Both basins have large negative SWE anomalies for type 1 years and about normal SWE for type 2 years. We also performed a similar analysis for TM over the two river basins (not shown) and found that for the Yakima River basin, the TM anomaly is strongly negative for type 1 years but is small (in absolute value) for type 2 years, whereas the Snake River basin has modest anomalies for both type 1 and type 2 years. These results are consistent with the fact that the Snake River is strongly snow dominant, whereas the Yakima River (whose headwaters are at lower elevation) is more affected by a combination of SWE and soil moisture. We infer that the inconsistencies (type 1 vs type 2) are associated with scale differences (regional vs basinwide) in the signature of droughts.

As noted in section 4, half of the SAD events are also among the 18 years with the most severe (low) hydropower generation. On the other hand, 1977, which appears in all of the other sector-specific indices, is not among the low hydropower generation years. We hypothesize that the reason may be the multiyear signature of the reservoir operating policy that determines the amount of hydropower generated each year. We examined this hypothesis by considering conditions in the preceding years in addition to the index year's hydropower generation. Figure 13 shows 1–6-yr-average January–August streamflow values, which are incorporated in the ColSim model operating decisions (Hamlet and Lettenmaier 1999). Figure 13 shows that for type 1 events, the average streamflow is higher than for type 2 in the index year; however, for the preceding years, type 1 streamflows are lower than for type 2. This result is consistent with the fact that the index year's hydropower depends not only on index year's streamflows, but also streamflow in the preceding years (which are not reflected in the SAD analysis, especially for single-year droughts like 1977).

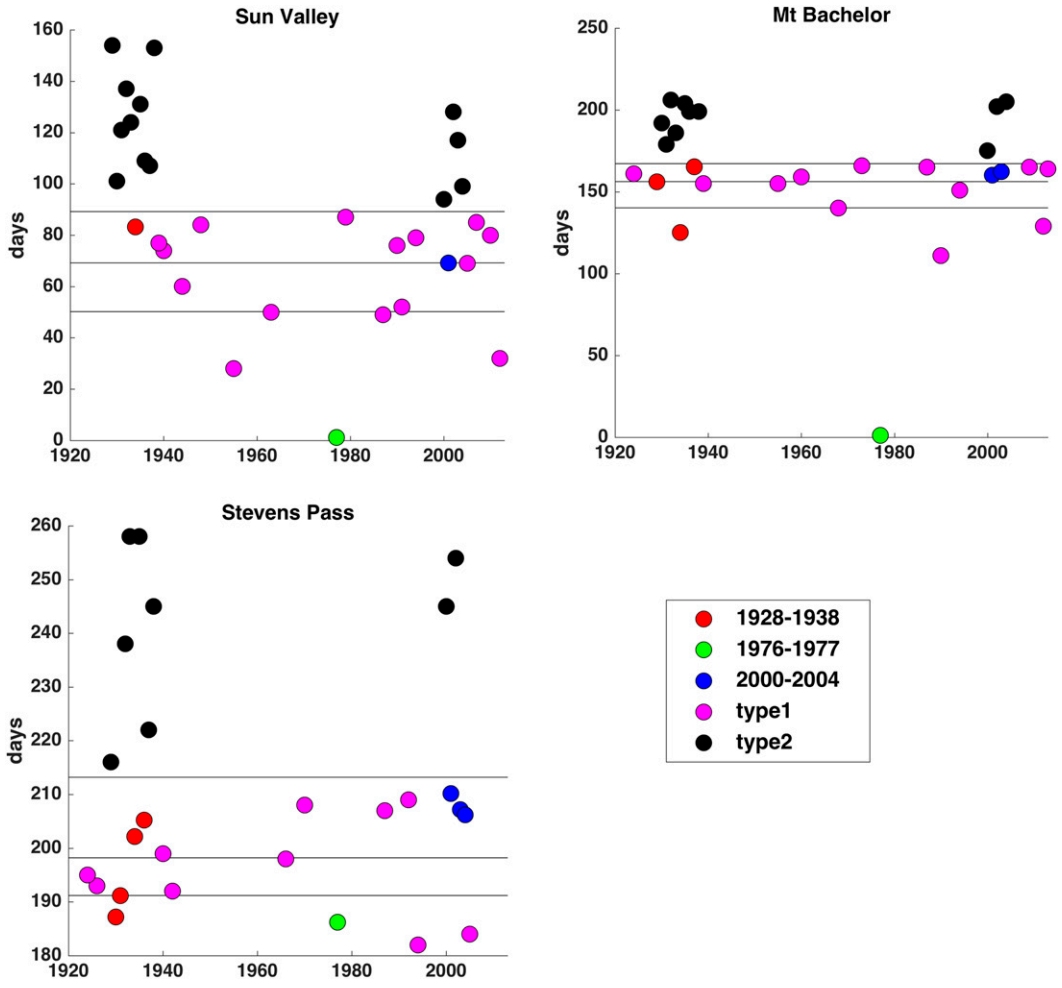

FIG. 11. As in Fig. 7, but for the number of days that experience low snow depth indices (as defined in section 4c) at (top left) Sun Valley, (top right) Mt Bachelor, and (bottom left) Stevens Pass ski areas.

For municipal water supply drought, all of the four water supply basins are on the western slope of the Cascade Mountains and snowmelt from their mountain headwaters contributes to their streamflow; although all are what is sometimes termed a transitional basin, meaning that their (annual) streamflows also have substantial rainfall contributions. In general, each of the basin's annual runoff (our water supply index) and (average annual) TM at the basin scale are highly correlated (range 0.80–0.90). We show regional TM anomaly bar plots for each river basin in Fig. 14. Clearly, type 1 events have much larger (negative) anomalies than do type 2 events. This suggests that type 1 and type 2 inconsistencies are largely related to spatial-scale differences between the regional SAD-based TM and the much smaller scale of the water supply basins. They may also be associated with subregional differences between the western part of the domain and the much larger area in the interior (east of the Cascades) portion of the region that dominates the TM values used in the SAD analysis.

The recreation index is based on model results for the single grid cells within which the ski areas are located, also resulting in potential mismatches between the large-region SAD TM and the local indices. SWE is

TABLE 1. Distribution of number of SAD drought events below given sector-specific threshold (numerator) and total number of SAD-derived drought years in each category (total number of SAD events = 16, or 16 × number of sites for multisite indices; this is the denominator for columns 3 and 4). Percentiles in column headers are for the sector-specific index distribution.

	<5%	<10%	<20%	>20%
Dryland agriculture	3/4	4/8	7/16	9/16
Irrigation	5/8	9/16	13/32	19/32
Hydropower	4/4	5/8	9/16	7/16
Municipal water supply	11/16	18/32	22/64	42/64
Recreation	5/12	8/24	16/48	32/48

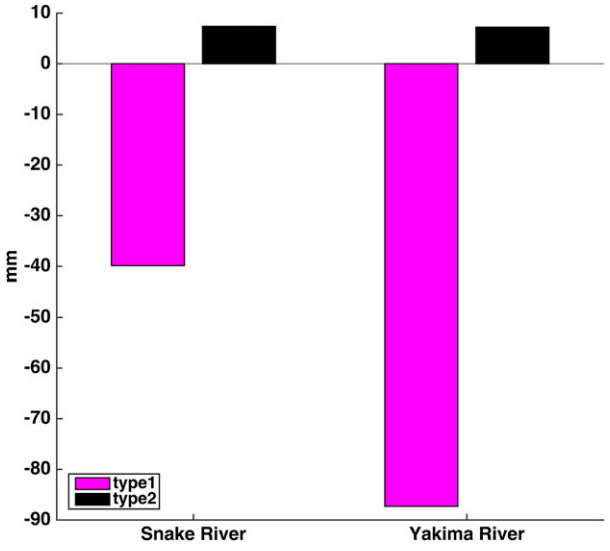

FIG. 12. SWE 1 Apr anomalies for type 1 and type 2 years for Snake River and Yakima River.

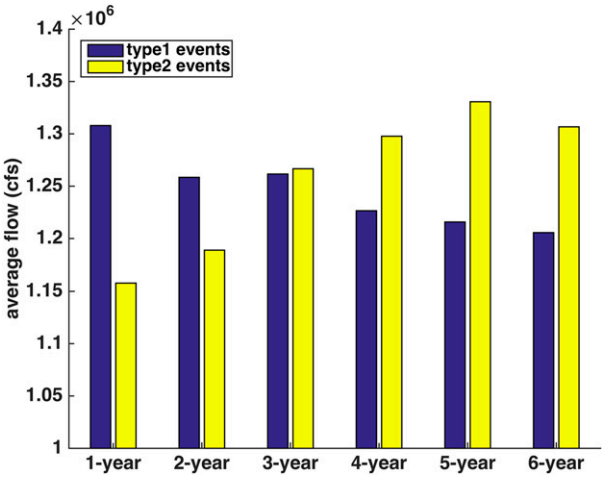

FIG. 13. Multiyear-average streamflow at the Dalles (downstream of major hydropower reservoirs; this is the control point for management of the Columbia River system) for type 1 and type 2 years.

largely controlled by accumulated winter precipitation (precipitation during the period from about 1 November to the beginning of melt—usually about 1 April) and also by winter temperature. The correlation coefficients between the snow-depth index and winter precipitation are 0.72, 0.76, and 0.72 for Sun Valley, Mt. Bachelor, and Stevens Pass, respectively. The correlation coefficients between the snow index and the number of days when the air temperature is below the model snow threshold (0.5°C) during winter are 0.34, 0.33, and 0.62. Winter precipitation, therefore, is the main controlling factor and winter temperature is secondary (although Stevens Pass, which is at lower elevation than the other two areas, is more sensitive to temperature than the other two sites). Figure 15 shows winter precipitation for type 1 and type 2 events. Type 1 events have much larger (negative) anomalies than do type 2 events. Therefore, inconsistencies between the regional SAD-based TM appear to be based primarily on 1) differences between water-year total precipitation and precipitation accumulated during the "core" winter season and 2) spatial-scale mismatches.

6. Summary and conclusions

We ran VIC for 1920–2013 over the PNW at 1/16° resolution. From the model output, we calculated TM percentiles and performed an SAD analysis to identify major TM droughts. We then evaluated drought severities using more specific measures appropriate to five sectors: dryland agriculture, hydropower, irrigated agriculture, water supply, and recreation (skiing). In all cases we investigated type 1 (sector-specific droughts not among the SAD years) and type 2 (SAD years not among the sector-specific droughts) inconsistencies between the regional and sector-specific droughts. Our main conclusions are as follows:

1) Three drought events account for almost all of the SAD space: the 1930s Dust Bowl drought (1928–38), the severe one-year 1977 drought, and the more recent 2000–04 event.
2) For the sector-specific droughts, the highest fraction of the most severe droughts (<0.05 percentile) occurred in SAD (regional) drought years, and the

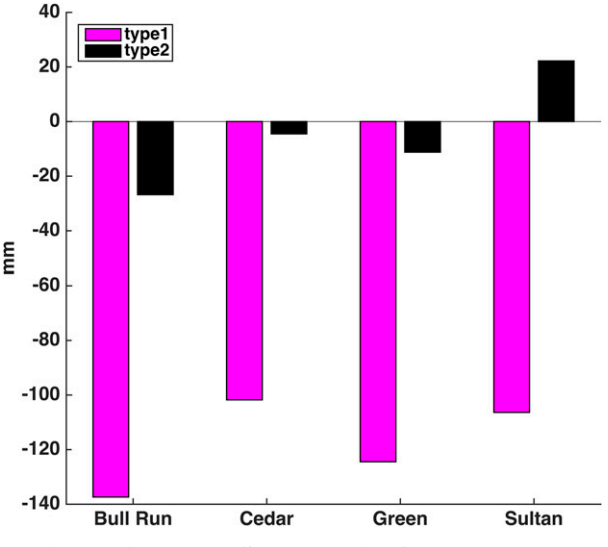

FIG. 14. Local TM anomalies for type 1 and type 2 years for four water supply rivers (Bull Run, Cedar, Green, and Sultan).

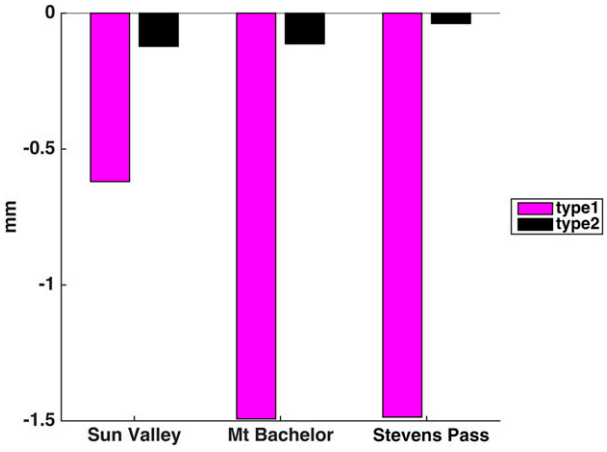

FIG. 15. Winter precipitation anomaly (November–March) for type 1 and type 2 years at three ski areas.

fractions generally declined at higher percentiles, that is, there were greater inconsistencies among the less severe sector-specific droughts.

3) In most cases, composites of the type 1 and type 2 inconsistencies suggest that they are attributable primarily to spatial-scale mismatches between the regional (SAD) and local scales on which the sector-specific indices were based, and to a lesser extent, to temporal differences. Differences among the variables (TM for SAD, and other variables, such as streamflow in the case of the irrigated agriculture and municipal water supply sectors) were less important, likely because these variables are highly correlated with TM at the regional scale.
4) The 1977 drought was prominent among all sector-specific indices except hydropower. The hydropower index (total hydropower generation) is unique in that it is a function not only of physical variables (regional streamflow) but also policy decisions (i.e., how much water to release from reservoirs), which depend not only on the current year's streamflow, but the one or two previous years. In this respect, while 1977 had exceptionally low runoff, more normal conditions prevailed in the previous (and subsequent) years, and for that reason 1977 was not among the lowest years of record for hydropower generation.

Acknowledgments. The work reported herein was supported by NOAA's Climate Program Office under Grant NA14OAR4310293 to the University of California, Los Angeles; the Joint Institute for the Study of the Atmosphere and Ocean (JISAO) under NOAA Cooperative Agreement NA10OAR4320148 (2010–15) and NA15OAR4320063 (2015–20), Contribution No. 2016-01-41 to the University of Washington; and NOAA RISA Award NA10OAR4310218 to Oregon State University with University of Washington as participant under subaward NA226B-D.

REFERENCES

Andreadis, K. M., and D. P. Lettenmaier, 2006: Trends in 20th century drought over the continental United States. *Geophys. Res. Lett.*, **33**, L10403, doi:10.1029/2006GL025711.

——, E. A. Clark, A. W. Wood, A. F. Hamlet, and D. P. Lettenmaier, 2005: Twentieth-century drought in the conterminous United States. *J. Hydrometeor.*, **6**, 985–1001, doi:10.1175/JHM450.1.

BPA, USBR, and USACE, 2001: The Columbia River system inside story. Tech. Rep., 80 pp. [Available online at https://www.bpa.gov/power/pg/columbia_river_inside_story.pdf.]

Cook, E. R., R. Seager, M. A. Cane, and D. W. Stahle, 2007: North American drought: Reconstructions, causes, and consequences. *Earth-Sci. Rev.*, **81**, 93–134, doi:10.1016/j.earscirev.2006.12.002.

Dilley, M., and B. N. Heyman, 1995: ENSO and disaster: Droughts, floods and El Niño/Southern Oscillation warm events. *Disasters*, **19**, 181–193, doi:10.1111/j.1467-7717.1995.tb00338.x.

Dracup, J. A., K. S. Lee, and E. G. Paulson, 1980: On the definition of droughts. *Water Resour. Res.*, **16**, 297–302, doi:10.1029/WR016i002p00297.

Fan, Y., and H. Van den Dool, 2004: Climate Prediction Center global monthly soil moisture data set at 0.5° resolution for 1948 to present. *J. Geophys. Res.*, **109**, D10102, doi:10.1029/2003JD004345.

Ferguson, S. A., 1999: Climatology of the interior Columbia River basin. USDA Tech. Rep. PNW-GTR-445, 40 pp. [Available online at http://www.fs.fed.us/pnw/pubs/gtr_445.pdf.]

Hamlet, A. F., and D. P. Lettenmaier, 1999: Effects of climate change on hydrology and water resources in the Columbia River basin. *J. Amer. Water Resour. Assoc.*, **35**, 1597–1623, doi:10.1111/j.1752-1688.1999.tb04240.x.

——, D. Huppert, and D. P. Lettenmaier, 2002: Economic value of long-lead streamflow forecasts for Columbia River hydropower. *J. Water Resour. Plann. Manage.*, **128**, 91–101, doi:10.1061/(ASCE)0733-9496(2002)128:2(91).

Kalnay, E., and Coauthors, 1996: The NCEP/NCAR 40-Year Reanalysis Project. *Bull. Amer. Meteor. Soc.*, **77**, 437–471, doi:10.1175/1520-0477(1996)077,0437:TNYRP.2.0.CO;2.

Knapp, P. A., P. T. Soulé, and H. D. Grissino-Mayer, 2004: Occurrence of sustained droughts in the interior Pacific Northwest (A.D. 1733–1980) inferred from tree-ring data. *J. Climate*, **17**, 140–150, doi:10.1175/1520-0442(2004)017<0140:OOSDIT>2.0.CO;2.

Lee, S.-Y., C. J. Fitzgerald, A. F. Hamlet, and S. J. Burges, 2011: Daily time-step refinement of optimized flood control rule curves for a global warming scenario. *J. Water Resour. Plann. Manage.*, **137**, 309–317, doi:10.1061/(ASCE)WR.1943-5452.0000125.

Liang, X., D. P. Lettenmaier, E. F. Wood, and S. J. Burges, 1994: A simple hydrologically based model of land surface water and energy fluxes for general circulation models. *J. Geophys. Res.*, **99**, 14 415–14 428, doi:10.1029/94JD00483.

Livneh, B., E. A. Rosenberg, C. Lin, B. Nijssen, V. Mishra, K. M. Andreadis, E. P. Maurer, and D. P. Lettenmaier, 2013: A long-term hydrologically based dataset of land surface fluxes and states for the conterminous United States: Update and extensions. *J. Climate*, **26**, 9384–9392, doi:10.1175/JCLI-D-12-00508.1.

Lohmann, D., E. Raschke, B. Nijssen, and D. P. Lettenmaier, 1998: Regional scale hydrology: II. Application of the VIC-2L model to the Weser River, Germany. *Hydrol. Sci. J.*, **43**, 143–158, doi:10.1080/02626669809492108.

Mao, Y., B. Nijssen, and D. P. Lettenmaier, 2015: Is climate change implicated in the 2013–2014 California drought? A hydrologic perspective. *Geophys. Res. Lett.*, **42**, 2805–2813, doi:10.1002/2015GL063456.

Mantua, N. J., S. R. Hare, Y. Zhang, J. M. Wallace, and R. C. Francis, 1997: A Pacific interdecadal climate oscillation with impacts on salmon production. *Bull. Amer. Meteor. Soc.*, **78**, 1069–1079, doi:10.1175/1520-0477(1997)078<1069:APICOW>2.0.CO;2.

Markoff, M. S., and A. C. Cullen, 2008: Impact of climate change on Pacific Northwest hydropower. *Climatic Change*, **87**, 451–469, doi:10.1007/s10584-007-9306-8.

Maybank, J., B. Bonsai, K. Jones, R. Lawford, E. G. O'Brien, E. A. Ripley, and E. Wheaton, 1995: Drought as a natural disaster. *Atmos.–Ocean*, **33**, 195–222, doi:10.1080/07055900.1995.9649532.

Mckee, T. B., N. J. Doesken, and J. Kleist, 1993: The relationship of drought frequency and duration to time scales. Preprints, *Eighth Conf. on Applied Climatology*, Anaheim, CA, Amer. Meteor. Soc., 179–184.

Mo, K. C., 2008: Model-based drought indices over the United States. *J. Hydrometeor.*, **9**, 1212–1230, doi:10.1175/2008JHM1002.1.

——, and D. P. Lettenmaier, 2014: Objective drought classification using multiple land surface models. *J. Hydrometeor.*, **15**, 990–1010, doi:10.1175/JHM-D-13-071.1.

Mote, P. W., A. F. Hamlet, M. P. Clark, and D. P. Lettenmaier, 2005: Declining mountain snowpack in western North America. *Bull. Amer. Meteor. Soc.*, **86**, 39–49, doi:10.1175/BAMS-86-1-39.

Narasimhan, B., and R. Srinivasan, 2005: Development and evaluation of soil moisture deficit index (SMDI) and evapotranspiration deficit index (ETDI) for agricultural drought monitoring. *Agric. For. Meteor.*, **133**, 69–88, doi:10.1016/j.agrformet.2005.07.012.

Palmer, W. C., 1965: Meteorological drought. U.S. Weather Bureau Research Paper 45, 58 pp. [Available online at http://www.ncdc.noaa.gov/temp-and-precip/drought/docs/palmer.pdf.]

Payne, J., A. Wood, and A. Hamlet, 2004: Mitigating the effects of climate change on the water resources of the Columbia River basin. *Climatic Change*, **62**, 233–256, doi:10.1023/B:CLIM.0000013694.18154.d6.

Scott, D., G. McBoyle, and A. Minogue, 2007: Climate change and Quebec's ski industry. *Global Environ. Change*, **17**, 181–190, doi:10.1016/j.gloenvcha.2006.05.004.

Seaber, P. R., F. P. Kapinos, and G. L. Knapp, 1987: Hydrologic unit maps. USGS Water-Supply Paper 2294, 66 pp. [Available online at http://pubs.usgs.gov/wsp/wsp2294/pdf/wsp_2294.pdf.]

Sheffield, J., 2004: A simulated soil moisture based drought analysis for the United States. *J. Geophys. Res.*, **109**, D24108, doi:10.1029/2004JD005182.

Shukla, S., and A. W. Wood, 2008: Use of a standardized runoff index for characterizing hydrologic drought. *Geophys. Res. Lett.*, **35**, L02405, doi:10.1029/2007GL032487.

——, A. C. Steinemann, and D. P. Lettenmaier, 2011: Drought monitoring for Washington State: Indicators and applications. *J. Hydrometeor.*, **12**, 66–83, doi:10.1175/2010JHM1307.1.

Steiger, R., and J. Stötter, 2013: Climate change impact assessment of ski tourism in Tyrol. *Tour. Geogr.*, **15**, 577–600, doi:10.1080/14616688.2012.762539.

Svoboda, M., and Coauthors, 2002: The Drought Monitor. *Bull. Amer. Meteor. Soc.*, **83**, 1181–1190, doi:10.1175/1520-0477(2002)083<1181:TDM>2.3.CO;2.

Tarhule, A., and P. J. Lamb, 2003: Climate research and seasonal forecasting for West Africans. *Bull. Amer. Meteor. Soc.*, **84**, 1741–1759, doi:10.1175/BAMS-84-12-1741.

USDA, 1997: Usual planting and harvesting dates for U.S. field crops. USDA Agricultural Handbook 628, 51 pp. [Available online at https://www.nass.usda.gov/Publications/Usual_Planting_and_Harvesting_Dates/uph97.pdf.]

Vano, J. A., M. J. Scott, N. Voisin, C. O. Stöckle, A. F. Hamlet, K. E. B. Mickelson, M. M. Elsner, and D. P. Lettenmaier, 2010: Climate change impacts on water management and irrigated agriculture in the Yakima River basin, Washington, USA. *Climatic Change*, **102**, 287–317, doi:10.1007/s10584-010-9856-z.

Wang, A., T. J. Bohn, S. P. Mahanama, R. D. Koster, and D. P. Lettenmaier, 2009: Multimodel ensemble reconstruction of drought over the continental United States. *J. Climate*, **22**, 2694–2712, doi:10.1175/2008JCLI2586.1.

——, D. P. Lettenmaier, and J. Sheffield, 2011: Soil moisture drought in China, 1950–2006. *J. Climate*, **24**, 3257–3271, doi:10.1175/2011JCLI3733.1.

Wood, A. W., and D. P. Lettenmaier, 2006: A testbed for new seasonal hydrologic forecasting approaches in the western U.S. *Bull. Amer. Meteor. Soc.*, **87**, 1699–1712, doi:10.1175/BAMS-87-12-1699.